

## Nanoporous Carbohydrate Metal–Organic Frameworks

Ross S. Forgan,<sup>†</sup> Ronald A. Smaldone,<sup>†</sup> Jeremiah J. Gassensmith,<sup>†</sup> Hiroyasu Furukawa,<sup>||</sup> David B. Cordes,<sup>⊥</sup> Qiaowei Li,<sup>||</sup> Christopher E. Wilmer,<sup>§</sup> Youssry Y. Botros,<sup>†,‡,‡,▽</sup> Randall Q. Snurr,<sup>§</sup> Alexandra M. Z. Slawin,<sup>⊥</sup> and J. Fraser Stoddart<sup>\*,†,○</sup>

<sup>†</sup>Center for the Chemistry of Integrated Systems, Department of Chemistry, <sup>‡</sup>Department of Materials Science, and <sup>§</sup>Department of Chemical & Biological Engineering, Northwestern University, 2145 Sheridan Road, Evanston, Illinois 60208-3133, United States

<sup>||</sup>The Center for Reticular Chemistry, Department of Chemistry and Biochemistry, University of California, Los Angeles, 607 Charles E. Young Drive East, Los Angeles, California 90095-1569, United States

<sup>⊥</sup>School of Chemistry, University of St. Andrews, Purdie Building, North Haugh, St Andrews, Fife, Scotland, KY16 9ST, United Kingdom

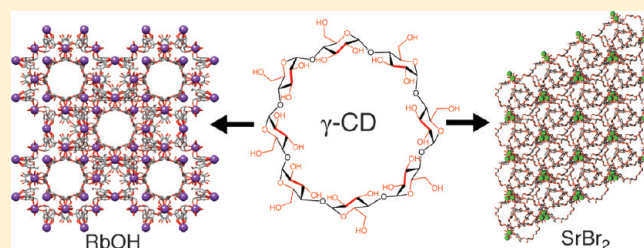
<sup>§</sup>Intel Laboratories, Building RNB-6-61, 2200 Mission College Boulevard, Santa Clara, California 95054-1549, United States

<sup>▽</sup>National Center for Nano Technology Research, King Abdulaziz City for Science and Technology, P.O. Box 6086, Riyadh 11442, Kingdom of Saudi Arabia

<sup>○</sup>NanoCentury KAIST Institute and Graduate School of EEWS (WCU), Korea Advanced Institute of Science and Technology (KAIST), 373-1, Guseong Dong, Yuseong Gu, Daejeon 305-701, Republic of Korea

**S** Supporting Information

**ABSTRACT:** The binding of alkali and alkaline earth metal cations by macrocyclic and diazamacrobicyclic polyethers, composed of ordered arrays of hard oxygen (and nitrogen) donor atoms, underpinned the development of host–guest supramolecular chemistry in the 1970s and 1980s. The arrangement of –OCCO– and –OCCN– chelating units in these preorganized receptors, including, but not limited to, crown ethers and cryptands, is responsible for the very high binding constants observed for their complexes with Group IA and IIA cations. The cyclodextrins (CDs), cyclic oligosaccharides derived microbologically from starch, also display this –OCCO– bidentate motif on both their primary and secondary faces. The self-assembly, in aqueous alcohol, of infinite networks of extended structures, which have been termed CD-MOFs, wherein  $\gamma$ -cyclodextrin ( $\gamma$ -CD) is linked by coordination to Group IA and IIA metal cations to form metal–organic frameworks (MOFs), is reported. CD-MOF-1 and CD-MOF-2, prepared on the gram-scale from KOH and RbOH, respectively, form body-centered cubic arrangements of ( $\gamma$ -CD)<sub>6</sub> cubes linked by eight-coordinate alkali metal cations. These cubic CD-MOFs are (i) stable to the removal of solvents, (ii) permanently porous, with surface areas of  $\sim 1200 \text{ m}^2 \text{ g}^{-1}$ , and (iii) capable of storing gases and small molecules within their pores. The fact that the –OCCO– moieties of  $\gamma$ -CD are not prearranged in a manner conducive to encapsulating single metal cations has led to our isolating other infinite frameworks, with different topologies, from salts of Na<sup>+</sup>, Cs<sup>+</sup>, and Sr<sup>2+</sup>. This lack of preorganization is expressed emphatically in the case of Cs<sup>+</sup>, where two polymorphs assemble under identical conditions. CD-MOF-3 has the cubic topology observed for CD-MOFs 1 and 2, while CD-MOF-4 displays a channel structure wherein  $\gamma$ -CD tori are perfectly stacked in one dimension in a manner reminiscent of the structures of some  $\gamma$ -CD solvates, but with added crystal stability imparted by metal–ion coordination. These new MOFs demonstrate that the CDs can indeed function as ligands for alkali and alkaline earth metal cations in a manner similar to that found with crown ethers. These inexpensive, green, nanoporous materials exhibit absorption properties which make them realistic candidates for commercial development, not least of all because edible derivatives, fit for human consumption, can be prepared entirely from food-grade ingredients.



### INTRODUCTION

Pedersen's seminal publications<sup>1</sup> in the *Journal of the American Chemical Society* in 1967 describing the accidental synthesis of an extensive range of macrocyclic polyethers he called crown ethers,<sup>2</sup> because of their ability to form strong complexes with alkali and alkaline earth metal cations, are widely recognized today as having marked a defining moment which led subsequently to the development by Lehn of a discipline he was later to call

supramolecular chemistry.<sup>3</sup> As the nascent field of crown ether chemistry<sup>4</sup> started to unfold around [18]crown-6 (Figure 1a) and its derivatives and analogues, for example, [2.2.2]cryptand (Figure 1b), Cram launched a rigorous new research program under the umbrella of host–guest chemistry.<sup>5</sup>

**Received:** August 31, 2011

**Published:** November 17, 2011

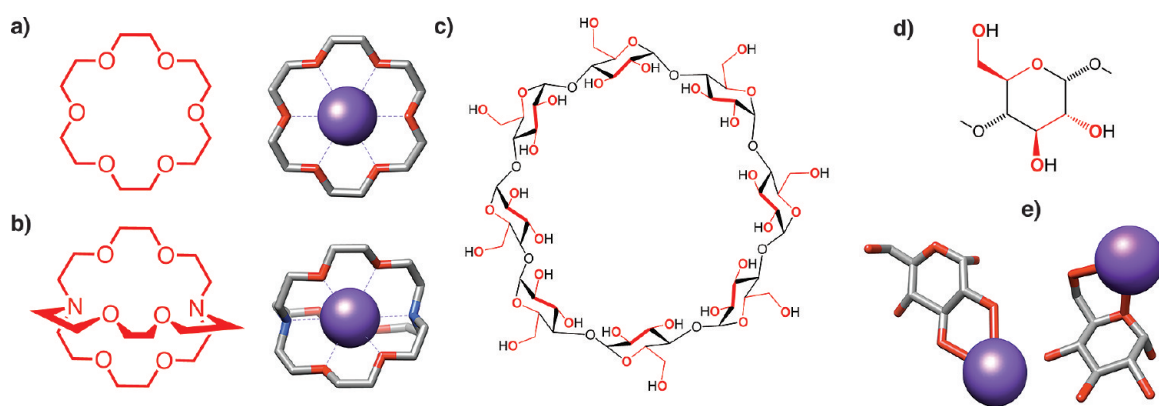


**Figure 1.** Examples of polyoxygenated compounds which can be used to coordinate to alkali or alkaline earth metal cations. In all cases, the  $-\text{OCCO}-$  or  $-\text{OCCN}-$  bidentate moieties, capable of chelation to hard Group IA and IIA metal cations, are colored red. (a) The structural formula of 18-crown[6], with a rendering of a crystal structure of its 1:1 complex with a  $\text{K}^+$  ion alongside. (b) The structural formula of [2.2.2]cryptand, and a rendering of a crystal structure of its 1:1 complex with a  $\text{K}^+$  ion alongside. (c) A conformational representation of  $\gamma$ -cyclodextrin ( $\gamma$ -CD) with its  $-\text{OCCO}-$  units on its primary and secondary faces colored red. (d) One of the eight  $\alpha$ 1,4-linked D-glucopyranosyl residues which comprise  $\gamma$ -CD, with the two possible  $-\text{OCCO}-$  coordination sites highlighted in red. (e) Renderings of the possible modes of coordination of  $\text{K}^+$  ions to the primary and secondary faces of a D-glucopyranosyl residue of  $\gamma$ -CD. Crystal structures were redrawn from CCDC depositions KOSRAL<sup>4f</sup> and KCRYPT10,<sup>6d</sup> respectively, with counterions and hydrogen atoms removed for clarity.

While [18]crown-6 was found to bind  $\text{K}^+$  ions in methanol with a stability constant ( $K_a$ ) in excess of  $10^6 \text{ M}^{-1}$ , diazamacrobicyclic polyethers like [2.2.2]cryptand were shown<sup>6</sup> by Lehn and Sauvage to exhibit  $K_a$  values<sup>7</sup> as high as  $10^{15} \text{ M}^{-1}$  for the binding of alkali metal cations in methanol. By contrast, the introduction by Cram<sup>5</sup> of axially chiral binaphthyl units into the crown-6 constitution played havoc with the ability of these hosts to form complexes in methanolic solution with Group IA metal cations for at least two reasons: (i) the disruption of the all-important  $-\text{OCH}_2\text{CH}_2\text{X}-$  ( $\text{X} = \text{O}, \text{N}$ ) repeating units present in [18]crown-6 and [2.2.2]cryptand by the binaphthyl units, and (ii) the replacement of the ethereal oxygen atoms by phenolic ones.<sup>8</sup> Our own early research<sup>9</sup> on the fusion of cyclohexane-1,2-diols and methyl 4,6-*O*-benzylidene- $\alpha/\beta$ -D-glycopyranosyl residues into the [18]crown-6 constitution revealed a marked dependence on the binding of alkali metal cations upon the conformation adopted by the crown ether. We discovered that access to the all-*gauche*  $D_{3d}$  conformation by the [18]crown-6 ring is not unimportant when it comes to its binding strongly to Group IA metal cations. Configurationally enforced perturbations<sup>10</sup> of the desirable stereoelectronic features provided by the highly symmetric crown conformation lead to  $K_a$  values of a considerably reduced magnitude compared with that of [18]crown-6. Irrespective of these not so subtle stereochemical considerations, the fact remains that a common feature of all these polyoxygenated ligands which bind alkali and alkaline earth metal cations are  $-\text{OCCO}-$  repeating units with *gauche* conformations defining their C–C bonds. This geometry orients the hard oxygen donors in a manner which allows them to interact with hard Group IA and IIA metal cations and is undoubtedly responsible for the strong pole–dipole interactions that lead cooperatively to large association constants for complexes incorporating a number of them. The question arises – can the stereoelectronics that have accounted for macrocyclic and diazamacrobicyclic polyethers binding strongly with alkali and alkaline earth metal cations be expressed at a higher level of (super)structure like those that constitute coordination polymers<sup>11</sup> and metal–organic frameworks (MOFs)?<sup>12</sup>

The fact that the  $-\text{OCCO}-$  binding motif is omnipresent (Figure 1c, d) in the cyclodextrins<sup>13</sup> would suggest that these

dissymmetric molecules could have a unique and prominent role to play in furthering the coordination chemistry of the alkali and alkaline earth metal cations. The fact that the  $\alpha$ 1,4-linked D-glucopyranosyl residues<sup>14</sup> which constitute the repeating units in these cyclic oligosaccharides display the  $-\text{OCCO}-$  binding motif on both their primary and secondary faces augurs well for their being able to form extended structures with Group IA and IIA metal cations.

With over a century of innovative and creative research on cyclodextrins contributing to the vastness of the scientific literature,<sup>15</sup> it is perhaps a little surprising that their coordinative chemistry with alkali and alkaline earth metal cations has not been investigated from a more rational viewpoint and raised to a much higher level of fundamental understanding with regard to their extended structures in the crystalline state. While there is little or no evidence, not surprisingly, in fact, that cyclodextrins bind alkali and alkaline earth metal cations strongly in aqueous solution, there are a number of solid-state structures in which the coordination of these cations by cyclodextrins has been observed. Both Group IA and IIA metal cations have been shown to link molecules of both  $\alpha$ -cyclodextrin ( $\alpha$ -CD) and  $\beta$ -cyclodextrin ( $\beta$ -CD) by coordinating (i) to their primary hydroxyl groups,<sup>16</sup> usually in concert with the contiguous glycosidic ring oxygen atoms, (ii) to their secondary hydroxyl groups,<sup>17</sup> or indeed (iii) to a combination<sup>18</sup> of both of these binding sites. The extensive range of coordination geometries which have been observed results presumably from the lack of preorganization of the numerous oxygen atoms that are capable of coordinating to the metal cations.

The chemistry and commercial potential of  $\gamma$ -cyclodextrin ( $\gamma$ -CD) has been much less intensively investigated compared to those of its smaller siblings,<sup>19</sup>  $\alpha$ -CD and  $\beta$ -CD, simply because, until quite recently,  $\gamma$ -CD was not commercially available at a cost that is affordable for carrying out experiments on greater than milligram scales.  $\gamma$ -CD has 8-fold symmetry<sup>20</sup> ( $C_8$ ) and a number of solid-state superstructures of it and its inclusion complexes adopt<sup>21</sup> highly symmetric tetragonal arrangements, usually in the somewhat rare  $P4_21_2$  space group. We discovered, quite by accident, that  $\text{K}^+$  ions form a highly porous, extended body-centered cubic structure when  $\gamma$ -CD is crystallized in aqueous



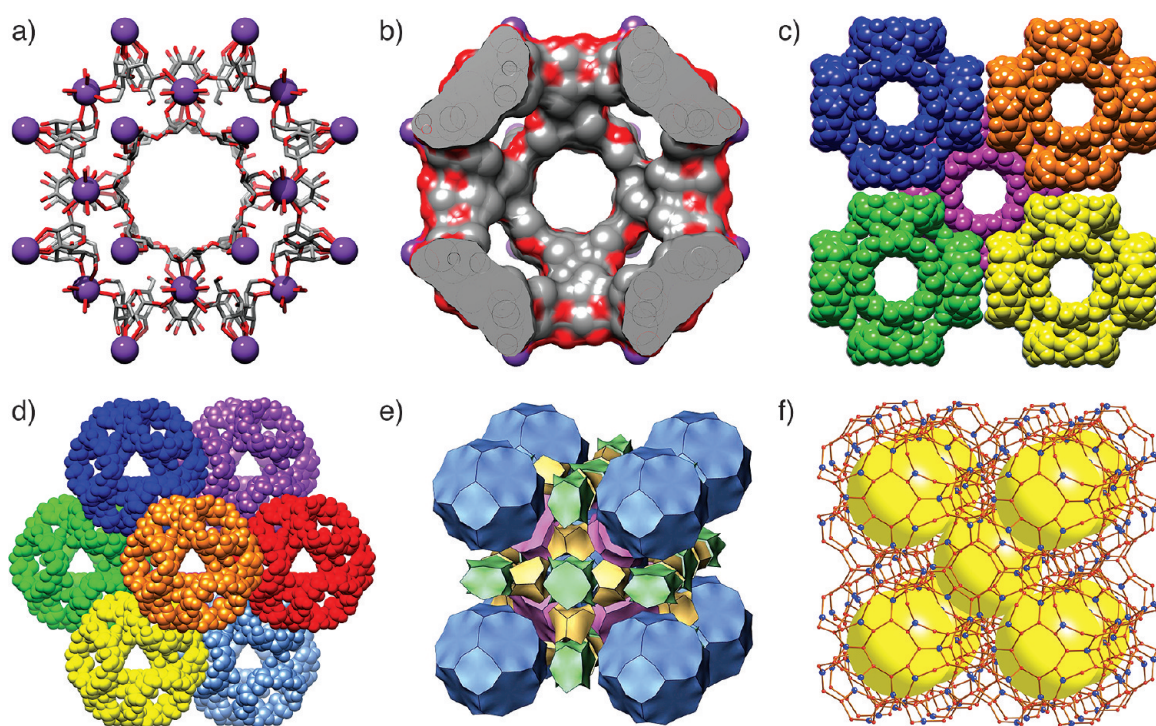


**Figure 2.** Representations of the solid-state structure of CD-MOF-1, which is isostructural with CD-MOF-2 and CD-MOF-3. (a) Tubular representations, with  $K^+$  ions represented as purple spheres of one of the repeating  $(\gamma\text{-CD})_6$  units, each of which houses a 1.7 nm diameter cavity. (b) A space-filling representation of one of the cubic  $(\gamma\text{-CD})_6$  units which has been cut away to reveal the hydrophobic inner spherical pore. (c) A space-filling representation of the extended body-centered cubic packing in the crystal structure of CD-MOF-1, wherein the spherical pores are connected by infinite channels defined by the inner diameter (0.78 nm) of the  $\gamma\text{-CD}$  tori. These channels propagate along the  $a$ ,  $b$ , and  $c$  crystallographic axes. Each of the separate  $(\gamma\text{-CD})_6$  units are colored individually to highlight the body-centered cubic packing arrangement. (d) A space filling representation of CD-MOF-1 as viewed at  $45^\circ$  to each of the crystallographic axes revealing the smaller 0.4 nm triangular channels. (e) A computer-generated illustration of the solvent accessible void spaces that are present in the CD-MOF extended structure. (f) The previously unknown *rra* crystallographic net, wherein the individual sugar units of the  $\gamma\text{-CD}$  ring are represented by red spheres, the  $K^+$  ions by blue spheres, and the large spherical cavities at the centers of the  $(\gamma\text{-CD})_6$  units as large yellow spheres.

methanol in the presence of potassium salts to give crystals with a cubic morphology. Here, in this full paper, we discuss (i) the serendipitous discovery of a highly porous crystalline compound composed of  $\gamma\text{-CD}$  tori and  $K^+$  ions, (ii) the generalization of this observation to include other alkali and alkaline earth metal cations, (iii) the characterization of these crystalline compounds as extended structures by single crystal X-ray diffraction analysis, (iv) their inclusion-forming properties toward counterions, solvents and small organic molecules, and (v) the ability of their extended structural frameworks to become activated in a manner that allows them to adsorb gases. The research was the subject of a preliminary communication<sup>22</sup> recently.

## RESULTS AND DISCUSSION

All the CD-MOFs discussed in this paper have been self-assembled using the same protocol (see section S2 in the Supporting Information for details). Eight equivalents of the alkali metal salt were dissolved in deionized water along with 1 equiv of  $\gamma\text{-CD}$ , usually at a concentration of 50 mM with respect to the cyclodextrin. Vapor diffusion of methanol into the aqueous solution resulted in the separation of crystals after approximately 2 days. When KOH and RbOH were used as the source of the alkali metal, colorless cubic crystals, up to 2 mm<sup>3</sup> in size and designated CD-MOF-1<sup>23</sup> and CD-MOF-2,<sup>24</sup> respectively, were isolated and analyzed (Figure 2) by single crystal X-ray diffraction.<sup>25,26</sup> These

two compounds, alongside CD-MOF-3,<sup>27,28</sup> prepared from  $\gamma\text{-CD}$  and CsOH, turned out to be isostructural, and comprise infinite body-centered frameworks of  $(\gamma\text{-CD})_6$  cubic units (Figure 2a) linked by alkali metal cations. The  $\gamma\text{-CD}$  macrocycles adopt the faces of a cube, with their primary faces pointing toward its interior and linked to one another by coordination of the alkali metal cations to the primary C-6 OH groups and the glycosidic ring oxygen atoms. An approximately spherical pore, of diameter 1.7 nm, resides (Figure 2d) at the center of the cube. The  $(\gamma\text{-CD})_6$  cubes pack in a body-centered cubic manner and are aligned perfectly along the  $a$ ,  $b$ , and  $c$  crystallographic axes (Figure 2c), connected by coordination of the alkali metal cations to the C-2 and C-3 OH groups on the outward-pointing secondary faces of the  $\gamma\text{-CD}$  tori.

The resultant channels, defined by the interior window (0.78 nm) of the  $\gamma\text{-CD}$  unit, link the central pores in all three dimensions. Further triangular channels, 0.4 nm in size, can be observed (Figure 2d,e) by orienting the structure at  $45^\circ$  to each of the crystallographic axes. These channels represent the snubbed “corners” of the  $(\gamma\text{-CD})_6$  units, and are again prolonged infinitely in three dimensions. The structure has a previously unseen topological net, *rra* (Figure 2f), which comprises the Schläfli symbol<sup>29</sup>  $(6^2.8)_4(6^4.8.10)_4$ , and defines a body-centered cubic network of large spherical pores, connected by numerous channels with a calculated 54% pore vacancy.

Each alkali metal cation is crystallographically equivalent, and participates in both (i) forming the  $(\gamma\text{-CD})_6$  cubes by bridging

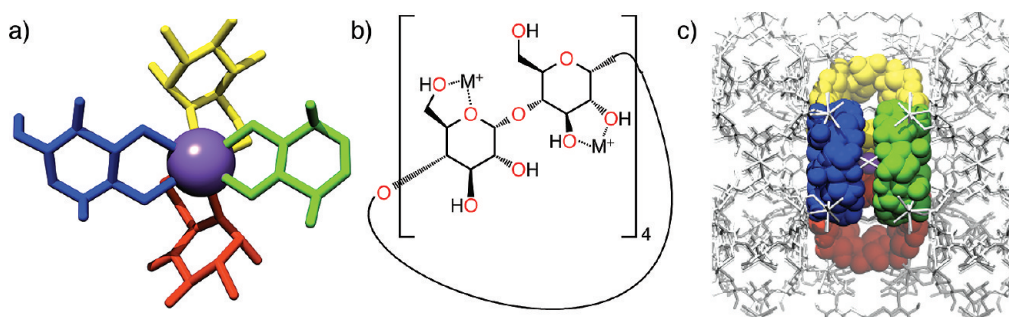


**Figure 3.** (a) Tubular representation of the coordination arrangement of the  $K^+$  ions (purple sphere) in the solid-state structure of CD-MOF-1. The  $K^+$  ion forms coordinative bonds to the secondary hydroxyl ions, attached to the C-2 and C-3 carbon atoms, of two individual  $D$ -glucopyranosyl residues (green and blue) while coordinating to the glycosidic ring oxygen and primary hydroxyl group attached to the C-6 carbon atom of two further residues (yellow and red). (b) The alternating arrangement of metal coordination to the primary and secondary face of each  $\gamma$ -CD in CD-MOF-1. (c) Expanded solid-state structure of CD-MOF-1, with four cyclodextrins coordinated to one  $K^+$  ion (purple sphere), displayed as space-filling models in green, blue, yellow, and red colors. The remainder of the framework is colored gray.

**Table 1. Bond Lengths (Å) around the Alkali Metal Cations in the Crystal Structures of CD-MOFs 1–3<sup>a</sup>**

	$M^+$	$M^+$ –primary OH	$M^+$ –ring O	$M^+$ –secondary OH	$M^+$ –secondary OH
CD-MOF-1	$K^+$	2.843(13)	2.824(6)	2.787(15)	2.954(10)
CD-MOF-2	$Rb^+$	3.046(7)	2.892(5)	2.909(8)	3.046(7)
CD-MOF-3	$Cs^+$	3.493(19)	3.077(9)	3.038(15)	3.125(18)

<sup>a</sup> While the metal cations are eight-coordinate (Figure 3), symmetry relates the two halves of the coordination sphere and, as such, there are four independent bond lengths, which result from coordination to a primary hydroxyl group (C6-OH), a glycosidic ring oxygen, and the two adjacent secondary hydroxyl groups (C2-OH and C3-OH).

two  $\gamma$ -CD tori at their primary faces and (ii) connecting these cubes by linking two further  $\gamma$ -CD units at their secondary faces. This dual linking results (Figure 3) in eight coordinate alkali metal cations that coordinate to the  $\gamma$ -CD units at each individual glucopyranosyl residue in an alternating primary face/secondary face pattern (Figure 3b,c).

The coordination spheres (Table 1) of the  $K^+$ ,  $Rb^+$ , and  $Cs^+$  cations of CD-MOFs 1–3, in turn, are similar, but with the expected increases in bond lengths as the ionic radii of the alkali metal cations grow as one descends Group IA of the Periodic Table.

The preparation<sup>23,24</sup> of CD-MOF-1 and CD-MOF-2 was facile and high yielding, with gram-scale quantities accessible on short time scales, thus allowing us to carry out a comprehensive study of their properties. The self-assembly<sup>27</sup> of CD-MOF-3 was complicated by the cocrystallization of a related polymorph, CD-MOF-4, which will be described in detail later. While it also proved possible<sup>22</sup> to prepare cubic crystals of space group *I432* and with a unit cell edge<sup>30</sup> of approximately 31 Å from various alkali metal salts (Table 2), full crystal structures were only be obtained for CD-MOFs 1–3, prepared from KOH, RbOH and CsOH, in turn. With the exception<sup>31</sup> of lithium salts, nearly all the alkali metal salts investigated form a cubic structure,<sup>32</sup> as evidenced by the collected unit cell data.<sup>33</sup>

We observed that the largest, best quality crystals were grown from solutions of basic salts, such as hydroxides and carbonates. Although these salts do not produce aqueous solutions of sufficient basicity to deprotonate the hydroxyl groups of  $\gamma$ -CD, they seem to facilitate crystal growth. We have also noted that crystals of CD-MOF-2, grown from RbOH, are the most robust of all crystals we have examined so far; they remain highly crystalline for months, even after removal from their mother liquors, allowing their manipulation and application in the

**Table 2. Alkali Metal Salts Employed in the Preparation of Cubic Single Crystals of Space Group *I432*, Alongside the Ratio of Metal Salt to  $\gamma$ -CD Used during Crystallization and the Unit Cell Edge Measured by Single Crystal X-ray Crystallography**

metal salt (MX)	MX: $\gamma$ -CD	unit cell edge/Å
KOH (CD-MOF-1)	1:8	31.006(8)
RbOH (CD-MOF-2)	1:8	31.079(1)
CsOH (CD-MOF-3)	1:8	30.868(10)
$Na_2CO_3$	1:8	30.751(9)
$K_2CO_3$	1:8	31.186(6)
KF	1:8	30.987(8)
$K_2$ (azobenzene-4,4'-dicarboxylate)	1:4	31.040(4)
KCl	1:8	31.161(9)
KBr	1:8	30.946(5)
NaBPh <sub>4</sub>	1:8	30.272(10)

micrometer-scale patterning of pH- and light-switchable molecules into their pores.<sup>34</sup>

It is also possible, by self-assembling them in solution in aqueous alcohol, to prepare CD-MOFs entirely from food-grade ingredients, namely, food-grade<sup>35</sup>  $\gamma$ -CD, potassium benzoate (E212, a preservative), water, and grain spirits (EtOH). In the solid-state structures of CD-MOFs 1–3, it did not prove possible to distinguish the hydroxide counterions from disordered interstitial water molecules, of which there are many. While the benzoate counterions are also expected to be disordered throughout the crystalline framework in the X-ray crystal structure<sup>36</sup> of the edible MOF, it proved possible to locate 50% of the benzoate anions in the solid-state structure (Figure 4a) of the edible MOF. Two crystallographically equivalent benzoate anions reside inside the



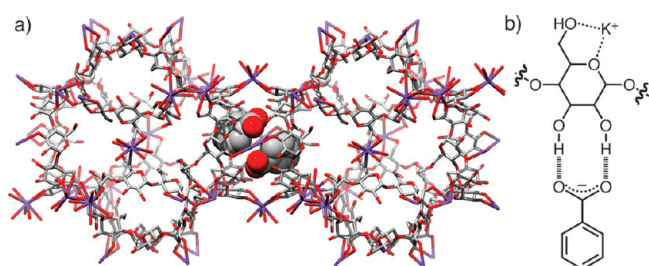


**Figure 4.** (a) Stick representation of the crystal structure of edible CD-MOF, showing the location of half of the benzoate anions, represented in space-filling mode, within the solid-state structure which is comprised of  $\gamma$ -CD and potassium benzoate. The resolved benzoate anions, identified within the  $\gamma$ -CD dimer, are located at the faces of each ( $\gamma$ -CD)<sub>6</sub> cube, and so each  $\gamma$ -CD molecule has a second benzoate anion inside its cavity. Benzoate anions are only displayed in one face-to-face dimer, and H atoms and solvent molecules are removed for clarity. (b) Schematic diagram indicating the nature of the hydrogen bonding between the carboxylate moiety of the benzoate anion and the C-2 and C-3 hydroxyl groups of the secondary face of one glucopyranosyl residue in the  $\gamma$ -CD torus.

$\gamma$ -CD “dimers” located at the faces of contiguous ( $\gamma$ -CD)<sub>6</sub> cubes and linked by the coordination of K<sup>+</sup> ions to the secondary faces of the two  $\gamma$ -CD units. Cyclodextrins are well-known<sup>13</sup> receptor molecules and, as such, CD-MOFs contain, in principle at least, numerous small molecule binding sites, or “sorting domains” within their extended frameworks.<sup>37</sup> Half of the benzoate anions are indeed located within the confines of these receptor molecules. Their orientation, however, is influenced by hydrogen bonding interactions (Figure 4b) from their carboxylate moieties to the C-2 and C-3 hydroxyl groups of a glucopyranosyl residue on the secondary face of the neighboring  $\gamma$ -CD unit.

The two H-bonds which form between each benzoate anion and each  $\gamma$ -CD unit have short O...O contacts, with distances of 2.58 and 2.69 Å, respectively, indicating that these noncovalent bonding interactions most certainly have a significant stabilizing effect on the location of the anions, overcoming the disorder which renders the locating of the remaining 50% of the benzoate anions nigh impossible. While  $\gamma$ -CD tori are capable, at least in aqueous solution, of hosting a prodigious variety of neutral and charged substrates by virtue of relatively strong interactions as a consequence of solvophobic/hydrophobic forces, the lack of bulk solvent, that is, H<sub>2</sub>O, within the CD-MOFs’ frameworks may be detrimental to this mode of binding of organic molecules in general in the cavities of the  $\gamma$ -CD tori that constitute the ( $\gamma$ -CD)<sub>6</sub> cubes.

The use of potassium benzoate, as well as dipotassium azobenzene-4,4’-dicarboxylate, as the metal ion source allows detection of all of the counterions in the framework after redissolving the CD-MOF in D<sub>2</sub>O and measuring the <sup>1</sup>H NMR spectrum. Potassium salts of both the monovalent benzoate anion and the divalent azobenzene-4,4’-dicarboxylate anion were used to prepare crystalline CD-MOFs (see Supporting Information, section S4). After 1 week, the mother liquors were decanted and the crystals were dissolved in D<sub>2</sub>O. In both cases, the <sup>1</sup>H NMR spectra (see Supporting Information, Figure S1) revealed the counterions were present in a ratio that would provide for a 2:1 ratio of K<sup>+</sup> ions to  $\gamma$ -CD tori, as measured in the solid-state structures, establishing that the counterions remained with the metal salts and confirming that deprotonation of the  $\gamma$ -CD tori does not occur within the extended CD-MOF structures.<sup>38</sup>

With gram-scale quantities of CD-MOF-1 and CD-MOF-2 to hand, we set about to determine if the frameworks could be evacuated and display permanent porosity, a necessary attribute of the compounds if they are to earn the distinction of being called MOFs. Interstitial solvents were exchanged by soaking crystals in CH<sub>2</sub>Cl<sub>2</sub> for 24 h, followed by vacuum drying to generate activated CD-MOFs. In order to determine the thermal stability of CD-MOFs 1 and 2, thermogravimetric analysis (TGA) was performed on both the as-synthesized and activated samples (see Supporting Information, S5).

The TGA traces (Figure 5a, b) show that CD-MOFs 1–2 are stable up to ca. 200 °C under oxidative conditions. Furthermore, these analyses demonstrate the efficiency of the activation process as there is no loss in mass before decomposition of the CD-MOF structure which, in the as-synthesized samples, is attributed to the expulsion of guest solvents trapped in the framework. The losses of solvent mass in both CD-MOFs 1 and 2 are also in very close agreement with the elemental analysis data for the as-synthesized and activated samples. To confirm sample integrity upon activation, powder X-ray diffraction analyses (Figure 5c, d) were carried out on activated samples of both compounds. Comparison of the diffraction patterns generated from the solid-state structures, in which solvent is not modeled, with those of the activated samples shows that the frameworks of CD-MOF-1 and CD-MOF-2 remain intact upon removal of occluded solvent.

The porosity and storage properties of activated samples of CD-MOF-2 were explored by performing gas sorption analyses (Figure 6) using nitrogen, hydrogen, carbon dioxide, and methane gases. The nitrogen isotherm shows a steep uptake in the low-pressure region at 77 K and a capacity of 250 cm<sup>3</sup> g<sup>-1</sup> at 1 bar, corresponding to a BET (Langmuir) surface area of 1030 (1110) m<sup>2</sup> g<sup>-1</sup> and pore volume of 0.47 g cm<sup>-3</sup>. The hydrogen isotherm demonstrates a modest storage ability of about 100 cm<sup>3</sup> g<sup>-1</sup> at 77 K at 1 bar. CD-MOF-2 also shows a steep rise in the low-pressure region of its carbon dioxide uptake isotherm taken at 298 K, indicative of a strong binding phenomenon.<sup>39</sup> Moreover, CD-MOF-2 reveals excellent selectivity for carbon dioxide over methane, as indicated by the poor uptake of CH<sub>4</sub> at 298 K. It should be noted that CD-MOF-1 exhibits very similar uptake behavior, with a measured BET (Langmuir) surface area of 1220 (1320) m<sup>2</sup> g<sup>-1</sup>. This is in stark contrast to  $\gamma$ -CD alone, which shows no uptake of N<sub>2</sub> or CO<sub>2</sub>.<sup>39</sup>

The interstitial water and alcohol molecules which are found in CD-MOFs after synthesis can be exchanged with nonpolar organic solvents allowing them to be exposed to solutions of organic molecules that are insoluble in aqueous solvent mixtures. The ability of the CD-MOF-2 to absorb small molecules into its structure postsynthetically was investigated by using the organic soluble dye molecule, 4-phenylazophenol (see Supporting Information, section S6). After soaking the CD-MOF-2 crystals in a saturated solution of the dye in CH<sub>2</sub>Cl<sub>2</sub> for three days, they were filtered, washed, and analyzed by <sup>1</sup>H NMR spectroscopy. Comparison of the integrals of the aromatic signals of the 4-phenylazophenol guest and the anomeric proton of the  $\gamma$ -CD units revealed a ratio of just over four molecules of 4-phenylazophenol per ( $\gamma$ -CD)<sub>6</sub> cube. Aqueous soluble guests, such as the dye Rhodamine B, can also be included within the framework by cocrystallization (see Supporting Information, section S7). Bright red crystals, confirmed to correspond to a cubic CD-MOF by single crystal X-ray diffraction measurement of the unit cell, were obtained when Rhodamine B was added to the initial aqueous solution used in the crystallization. Dissolution of these crystals

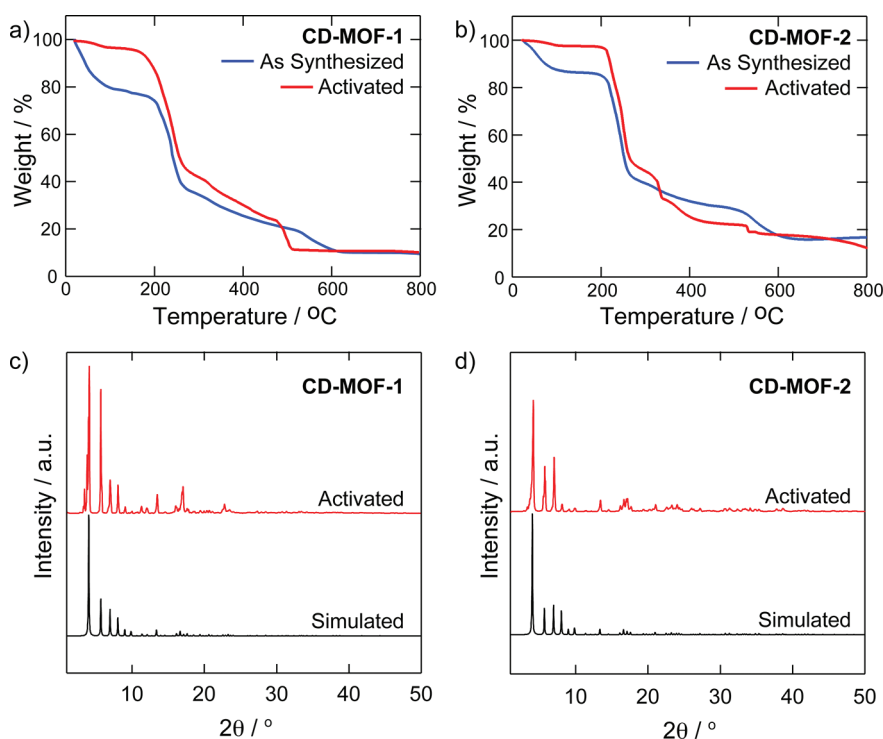


**Figure 5.** Thermogravimetric analytical traces of (a) CD-MOF-1 and (b) CD-MOF-2 in both their as-synthesized (blue lines) and activated (red lines) forms. In both as-synthesized samples, considerable mass loss, in the form of interstitial crystallization solvents, occurs in the low temperature region. Very little solvent remains in the activated samples, observations which show mass losses commensurate with the elemental analysis data. In all samples, further mass loss, attributed to oxidative degradation of the  $\gamma$ -CD units, occurs at approximately 180 °C. Powder X-ray diffraction analyses of activated (c) CD-MOF-1 and (d) CD-MOF-2 compared to patterns simulated from their respective single crystal structures, which do not model interstitial solvents. The similarity of the theoretical and experimental patterns indicates that the frameworks are stable to the activation process.

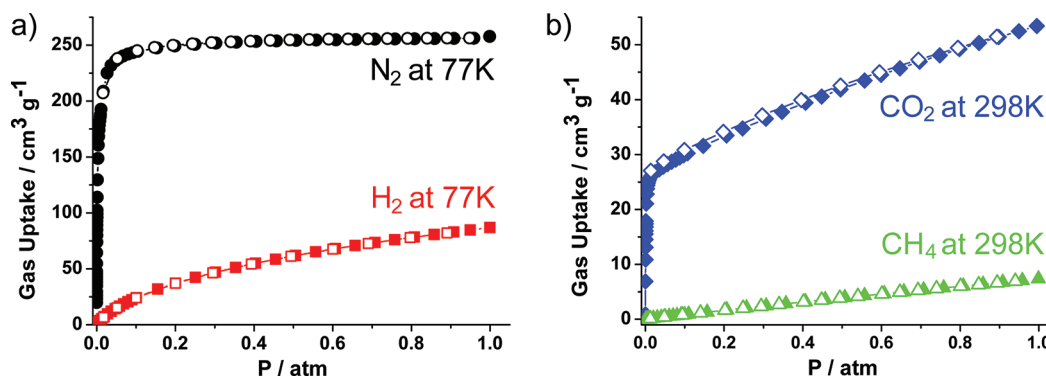


**Figure 6.** Adsorption isotherms measured on activated CD-MOF-2 for the uptake of (a) N<sub>2</sub> (black circles) and H<sub>2</sub> (red squares) at 77 K and (b) CO<sub>2</sub> (blue diamonds) and CH<sub>4</sub> (green triangles) at 298 K. Filled and open symbols represent sorption and desorption traces, respectively, while connecting lines are for guidance only. The N<sub>2</sub> uptake defines a BET (Langmuir) surface area of 1030 (1110) m<sup>2</sup> g<sup>-1</sup>.

in D<sub>2</sub>O, followed by <sup>1</sup>H NMR spectroscopic analysis, once again revealed that approximately four molecules of Rhodamine B reside within one ( $\gamma$ -CD)<sub>6</sub> cube.

The ease of synthesis of CD-MOF-1 and CD-MOF-2 were key to allowing us to examine their properties in considerable detail. Complications arose, however, when salts of Na<sup>+</sup> and Cs<sup>+</sup> were employed in the crystallization of CD-MOFs, on account of the fractional crystallization of other related extended structures. For example, in the case of CsOH during the growing of cubic crystals of CD-MOF-3, we observed the formation of another distinct crystalline form with a very different morphology from

that of the large cubes which are characteristic of CD-MOF-3 crystals. These fine, needle shaped crystals have been characterized by X-ray diffraction,<sup>40</sup> revealing (Figure 7) that they have a channel-type structure, which we have termed CD-MOF-4, consisting of  $\gamma$ -CD tori linked to one another through Cs<sup>+</sup> ions coordination to form channels along the crystallographic *c* axis.

In CD-MOF-4, Cs<sup>+</sup> ions link the cyclodextrins in a head-to-tail, that is, primary face to secondary face, fashion along the *c* axis, in addition to linking these stacks of  $\gamma$ -CD molecules in a checkerboard-like arrangement (Figure 7a) in the *ab* plane. The packing arrangement of these metal-linked  $\gamma$ -CD channels leads

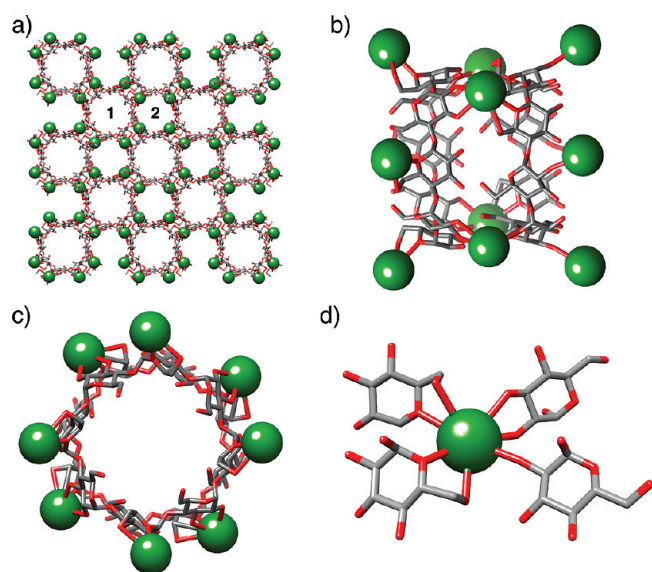


**Figure 7.** (a) Crystal packing of CD-MOF-4 viewed down the crystallographic  $c$  axis. (b) Side-on view showing the primary face orientation of the  $\gamma$ -CD rings in the extended structure. (c) Top view of the arrangement of  $\text{Cs}^+$  ions around two  $\gamma$ -CD units. This view illustrates the  $12^\circ$  offset of the  $\text{Cs}^+$  ions along the channels. (d) Coordination sphere of the  $\text{Cs}^+$  ions which has been simplified to show only the  $\text{D}$ -glucopyranosyl residues that are directly coordinating to the  $\text{Cs}^+$  ion.

to the formation (Figure 7a) of two different channel types, one which is defined by the inner cavities (0.78 nm in diameter) of the  $\gamma$ -CD tori forming stacks, labeled as **1**, and another, **2**, which is defined by the interstitial spaces (0.7 nm) between the  $\gamma$ -CD channels. While the  $\gamma$ -CDs align to form perfect, infinite channels, the macrocycles themselves are torsionally offset (Figures 7b and 7c) from one another by approximately  $12^\circ$ .

In comparison with the crystal superstructures<sup>21</sup> of  $\gamma$ -CD solvates, in which  $\gamma$ -CD molecules adopt a similar stacked arrangement along the  $c$  axis to that observed in CD-MOF-4, the presence of the linking  $\text{Cs}^+$  ions in the latter adds considerable stability to the crystals. While Steiner and Saenger<sup>21</sup> reported the high sensitivity of  $\gamma$ -CD solvate crystals to solvent loss, crystals of CD-MOF-4 are extremely stable when they are removed from their mother liquors. The  $\text{Cs}^+$  ions also link the  $\gamma$ -CD units in a very regular head-to-tail array in CD-MOF-4, whereas other known  $\gamma$ -CD solvate superstructures have the head-to-head/tail-to-tail/head-to-tail repeating motif (i.e., primary-to-primary, secondary-to-secondary, and then primary-to-secondary in a repeating fashion). This increased stability and ordering of  $\gamma$ -CD tori in the crystalline CD-MOF-4 has implications if the nano-channel extended structure is to find application, for example, as a stationary phase for chromatography.<sup>41</sup>

Interestingly, the pattern (Figure 7b,c) of metal coordination around the  $\gamma$ -CD tori in CD-MOF-4 is very similar to those observed in CD-MOF-1–3, wherein each  $\text{D}$ -glucopyranosyl residue is oriented in alternating fashion in coordination with ions that are between the primary and secondary faces. The environments around the  $\text{Cs}^+$  ions differ, however, in both geometry as well as coordination number. The metal ions are seven-coordinate (Figure 7d) and are bonded to four  $\gamma$ -CD tori through two glycosidic oxygen atoms, two primary and three secondary hydroxyl groups, rather than the four observed in the case of CD-MOF-3.

There also appears to be a considerable amount of free space in the coordination sphere surrounding the  $\text{Cs}^+$  ions, where hydroxide counterions, water molecules, or other solvents could potentially reside, particularly since the free space is oriented toward the interstitial channel **2**. No experimental evidence for this proposal, however, could be gleaned from the X-ray diffraction data.

Topological analysis of the three-dimensional network formed by CD-MOF-4 indicates that it comprises two different nodes. One of these is three-connected, and based on the individual  $\text{D}$ -glucopyranosyl residues of the  $\gamma$ -CD units, while the other is six-connected, and based on the  $\text{Cs}^+$  ions, in a similar manner to the **rra** network formed by CD-MOF-3. The resulting network has not previously been identified, and has the Schläfli symbol<sup>23</sup>  $(6.8^2)_4(6^2.8^2.10^2)$ . Not surprisingly, perhaps, in isomeric extended network structures, strong similarities are observed between the topology of the structure of CD-MOF-4 and that of CD-MOF-3. Both nets show three- and four-connected nodes in equivalent ratios, while rings of the same sizes make up the networks. The distinction between the networks arises in the relative amounts of the different sized rings, with CD-MOF-4 showing more eight- and ten-membered rings, emanating from the stacking of the  $\gamma$ -CD rings atop of each other, while CD-MOF-3 has more six-membered rings, generated by the connection of the cuboctahedral cages within the net.

Despite the fact that both CD-MOF-3 and CD-MOF-4 crystallize together during the same crystal growing experiments, their different crystal habits — large polyhedra and long needles, respectively — mean that manual separation of the crystals is possible. Attempts to activate a sample of separated cubic CD-MOF-3 employing the same approach as used previously for CD-MOF-1 and CD-MOF-2, that is, soaking in  $\text{CH}_2\text{Cl}_2$  followed by removal of solvent under vacuum, lead to some degree of degradation of the framework, to the extent that the measurement of porosity by  $\text{N}_2$  absorption has not been carried out in a successful manner. The channel-like structure of CD-MOF-4, however, is stable to the activation process, and a modest surface area of  $376 \text{ m}^2 \text{ g}^{-1}$  has been calculated by the Langmuir ( $339 \text{ m}^2 \text{ g}^{-1}$  by BET) method, based on the  $\text{N}_2$  adsorption isotherm measured at 77 K. The lower surface area value is not unexpected, since CD-MOF-4 has a more dense structure. Nevertheless, its stability and porosity, combined with its one-dimensional channel structure, augur well for potential applications in separation science and technology.

The two polymorphs can also be distinguished by the manner in which the  $\text{Cs}^+$  ions distribute themselves around the  $\gamma$ -CD rings. In CD-MOF-4, each  $\gamma$ -CD unit is sandwiched between two sets of  $\text{Cs}^+$  ions that are all equidistant from the center of the ring, whereas in CD-MOF-3, there are four “inner”  $\text{Cs}^+$  ions which are closer to the center of the  $(\gamma\text{-CD})_6$  unit, with the other four “outer”  $\text{Cs}^+$  ions being positioned further away from the center. Predicting which polymorph will dominate in a crystal growth experiment is typically not straightforward since the outcome is influenced by kinetic as well as thermodynamic considerations.<sup>42</sup> One strategy for predicting which polymorph is *kinetically* more favorable might entail determining the expected distribution of  $\text{Cs}^+$  ion positions relative to bound  $\gamma$ -CD rings in solution, which would subsequently “seed” the corresponding solid phase. For example, for a single  $\gamma$ -CD molecule in solution, it is not unlikely that both possible arrangements of  $\text{Cs}^+$  ions are enthalpically more or less the same, while the asymmetrical “inner-outer” arrangement is entropically preferred because of the greater



degrees of freedom expressed at this level. This scenario would lead to the macroscopic growth of CD-MOF-3, despite the fact that it might be thermodynamically disfavored relative to the channel-forming morphology of CD-MOF-4.

In order to determine which polymorph is more *thermodynamically* favorable, we have calculated the lattice energies of each by modeling the forces between the atoms using the Universal Force Field<sup>43</sup> and taking into account electrostatic interactions, summed by the Ewald method.<sup>44</sup> The latter were modeled by partial point charges at the atomic centers, derived using the charge equilibration method.<sup>45</sup> The calculated enthalpic difference between the two polymorphs is  $\sim 8 \text{ kJ mol}^{-1}$  per  $(\text{CsOH} \cdot \text{C}_{24}\text{H}_{40}\text{O}_{20})$  unit, favoring the more tightly packed channel-forming structure of CD-MOF-4. This difference in enthalpies is similar to those found in polymorphs of crystallized pharmaceutical compounds.<sup>46</sup> Applying increasingly larger external pressures leads, in the calculations, to an increase in the difference between the enthalpies, from an additional  $20 \text{ kJ mol}^{-1}$  at 1000 bar to  $100 \text{ kJ mol}^{-1}$  at 5000 bar, suggesting that it might be possible to generate one polymorph selectively in preference to the other. Future computational studies could clearly be directed at achieving a more detailed understanding of the nature of CD-MOF formation and the elucidation of concrete design rules for creating novel porous CD-based structures.

A similar situation arises when salts of  $\text{Na}^+$  are used as the source of the alkali metal ions. Attempts to prepare cubic CD-MOFs from different  $\text{Na}^+$  sources led to different outcomes, based on the choice of the counterion. When  $\text{Na}_2\text{CO}_3$  was employed, cubic crystals were obtained with a unit cell edge of approximately  $31 \text{ \AA}$  and an  $I432$  space group. Although we have not been successful in our attempts so far to complete the refinement of the solid-state structure to state acceptable for publication in the literature using data collected from these crystals, we have been able to conclude, from the diffraction data, that they comprise a cubic CD-MOF structure.

When  $\text{NaOH}$  was employed as the source of  $\text{Na}^+$  ions, a channel-type solid-state structure,  $[(\text{NaOH})_2 \cdot (\gamma\text{-CD})]_n$ , was obtained (Figure 8a, b) with an alignment of  $\gamma\text{-CD}$ s similar to that observed in the  $\text{CsOH}$  isomorph, CD-MOF-4. In this case, rather than witnessing a perfect alignment of the channels down the crystallographic  $c$  axis, they are stacked (Figure 8b) in an offset manner down the  $a$  axis. The  $\gamma\text{-CD}$  tori themselves are connected to one another by  $\text{Na}^+$  ions coordinated only to their secondary faces, resulting in tail-to-tail pairs of  $\gamma\text{-CD}$  tori which are joined by yet more  $\text{Na}^+$  ions in two-dimensional sheets, forming a square-grid network (**sql**).<sup>47</sup> The two-dimensional sheets are aligned in an offset manner, with the primary faces of the  $\gamma\text{-CD}$  tori facing each other, although not coordinated by any  $\text{Na}^+$  ions.

There are two types of  $\text{Na}^+$  ions in  $[(\text{NaOH})_2 \cdot (\gamma\text{-CD})]_n$ , both of which are six coordinate, with pseudo-octahedral coordination spheres. The first is similar to the cations in the other CD-MOF structures and their isomorphs insofar as the ions are bound (Figure 8c) to four separate  $\gamma\text{-CD}$  tori. Absent, however, are the interactions with either the primary hydroxyl groups or glycosidic ring oxygen atoms which have been observed in previous structures. In this case, the ions are only involved in binding to secondary hydroxyl groups, namely, four C-2 hydroxyl groups and two of the C-3 variety. Although the second  $\text{Na}^+$  ion has a similar coordination geometry, it is bound to only three oxygen atoms from three separate secondary hydroxyl groups on distinct  $\gamma\text{-CD}$  tori, and three further lone oxygen atoms. Since these latter oxygen atoms are not associated with any of the  $\gamma\text{-CD}$  tori, we posit that these are most likely water molecules or

hydroxide counterions that are incorporated during the crystal formation (Figure 8d). The smaller radius of the  $\text{Na}^+$  cation, coupled with the fact that these hydroxide counterions are disposed toward coordinating to  $\text{Na}^+$  ions in this fashion, may be responsible for the formation of this structural alternative to the cubic CD-MOF.

In all the examples of CD-MOFs and other extended frameworks hitherto presented, the cation employed was provided in the form of the salt of an alkali metal. Equipped with the diversity of structural arrangements from this group of monovalent metals, we decided to examine the structures obtained when other salts, in particular divalent species, were crystallized using the same protocol in the presence of  $\gamma\text{-CD}$ . A survey of the alkaline earth metals revealed only one set of crystals suitable for single-crystal diffraction analysis, isolated from aqueous solutions containing  $\gamma\text{-CD}$  and  $\text{SrBr}_2$ . Repeated experiments, wherein diffusion of  $\text{MeOH}$  into aqueous mixtures of  $\text{SrBr}_2$  and  $\gamma\text{-CD}$  were attempted, resulted in the isolation of only one or two crystals, which could be analyzed by X-ray diffraction analysis, from each experiment. The structure of  $[(\text{SrBr}_2) \cdot (\gamma\text{-CD})]_n$  turned out to be markedly different from the cubic and channel topologies obtained with the alkali metals. The  $\gamma\text{-CD}$  tori are arranged spatially in a trigonal "slipped stack" configuration (Figure 9a), producing a convoluted and nonlinear channel structure which runs along the  $c$  axis in an infinite manner. The channel structure is punctuated by large cavities inside the crystal structure with maximum and minimum diameters of  $6.8$  and  $3.2 \text{ \AA}$ , respectively.

The accessible void space was calculated in two steps. First, the inaccessible volume was defined from the union of spheres of a size equal to the van der Waals radii of the framework atoms added to the radius of a theoretical solvent molecule, assumed to be spherical, on a 3D mesh with a resolution of  $0.5 \text{ \AA}$ . Second, this volume was subtracted from the parallelepiped defined by the unit cell to obtain the void volume. The calculations were carried out with the Blender<sup>48</sup> software package using the Void Analyzer module.<sup>49</sup>

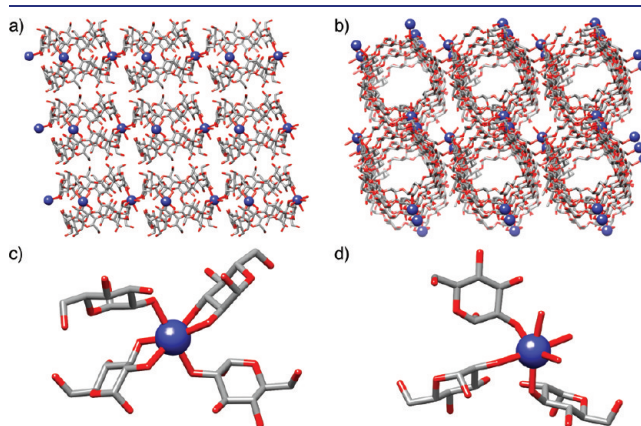


**Figure 8.** At the top are illustrations of the solid-state extended structure of  $[(\text{NaOH})_2 \cdot (\gamma\text{-CD})]_n$ . Each illustration shows the cyclodextrin tori as stick models and the sodium ions as blue spheres. Side-on (a) and top-down (b) views of the packing arrangement of the  $\text{NaOH}$  polymorph. At the bottom are portrayals of the coordination environment around the two independent  $\text{Na}^+$  ions observed in the  $\text{NaOH}$  isomorph. Although both  $\text{Na}^+$  ions have pseudo-octahedral coordination spheres, they differ in that one (c) ion type coordinates to four  $\gamma\text{-CD}$  tori while the other (d) coordinates to three  $\gamma\text{-CD}$  tori, as well as three interstitial oxygen atoms thought to be  $\text{OH}^-$  counterions or  $\text{H}_2\text{O}$  molecules.



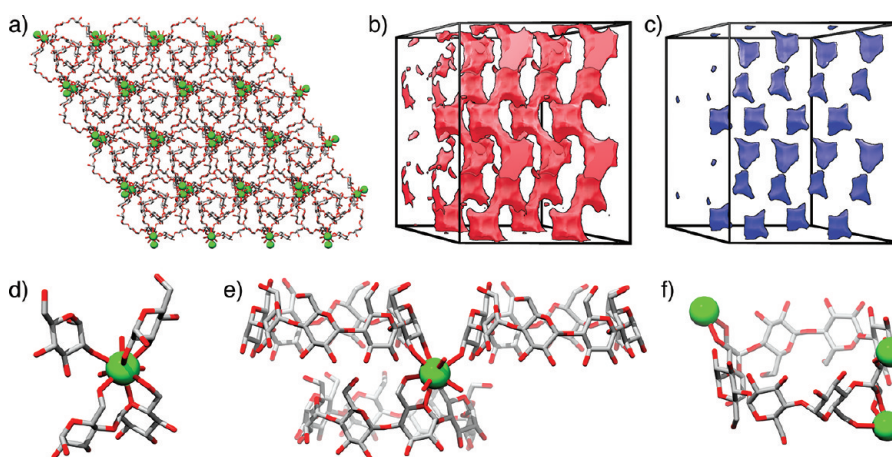


**Figure 9.** Solid-state structure of  $[(\text{SrBr}_2) \cdot (\gamma\text{-CD})]_n$ . (a) A stick diagram of the crystal packing viewed down the crystallographic  $c$  axis, with  $\text{Sr}^{2+}$  ions represented as green spheres. (b) The channels (red) that run down the crystallographic  $c$  axis, visualized by calculating the solvent accessible pore space for a spherical molecule of radius 1 Å, bound within a parallelepiped that corresponds to a supercell of  $2 \times 2 \times 2$  unit cells. (c) The calculated voids (blue) accessible to a spherical molecule of 1.85 Å radius, which corresponds well to the size of the  $\text{N}_2$  molecule, showing that  $[(\text{SrBr}_2) \cdot (\gamma\text{-CD})]_n$  is not likely to be porous to gases such as  $\text{N}_2$ . (d) The coordination of  $\text{Sr}^{2+}$  ions in the solid-state structure of  $[(\text{SrBr}_2) \cdot (\gamma\text{-CD})]_n$ . The  $\text{Sr}^{2+}$  ion is found to be nine-coordinate, while (e) each metal coordinates to three  $\gamma\text{-CD}$  tori (via six Sr–O bonds) and three molecules of water. (f) The  $\gamma\text{-CD}$  tori are coordinated to three  $\text{Sr}^{2+}$  ions each.

For a theoretical spherical molecule with a radius of only 1 Å, solvent accessible channels (Figure 9b) run down the crystallographic  $c$  axis of  $[(\text{SrBr}_2) \cdot (\gamma\text{-CD})]_n$ . On going, however, to a spherical molecule with a radius of 1.85 Å, which approximates well with  $\text{N}_2$  (Figure 9c), the solvent accessible voids are considerably smaller and disparate from one another. These disconnected cavity spaces indicate that  $[(\text{SrBr}_2) \cdot (\gamma\text{-CD})]_n$  is unlikely to be capable of absorbing gases of a size similar to  $\text{N}_2$ . The bromide counterions which, in this case, are well-ordered and resolved crystallographically, occupy space within the smaller diameter corridors. Owing to the large radius of bromide anions, these narrow corridors are likely to impart hindrance to potential gas uptake by the species. On account of these experimentally observed and theoretically implied factors, allied with the particularly low yield resulting from the crystallization process, the gas uptake of this framework was not investigated further.

Analysis of the structure of  $[(\text{SrBr}_2) \cdot (\gamma\text{-CD})]_n$  reveals the cation coordination to be different from those present in the structures where the  $\gamma\text{-CD}$  tori are bound to alkali metal cations. The  $\text{Sr}^{2+}$  cations are nine-coordinate species (Figure 9d), triply occupied by water and bound to three individual  $\gamma\text{-CD}$  units (Figure 9e). One  $\text{Sr}^{2+}$  cation binds to two  $\text{D}$ -glucopyranosyl residues on a single  $\gamma\text{-CD}$  torus, using two primary hydroxyl groups and one glycosidic ring oxygen atom. The single bond between the glycosidic oxygen atom and the metal center is 2.75 Å in length, while the Sr–O distances between the two primary hydroxyl groups are 2.58 and 2.65 Å. Two further  $\gamma\text{-CD}$  rings coordinate to the  $\text{Sr}^{2+}$  cation through their primary hydroxyl groups, forming bonds between 2.61 and 2.68 Å in length; there are no bonds to the secondary faces of the  $\gamma\text{-CD}$  tori. These bond distances to the dicationic  $\text{Sr}^{2+}$  ions are slightly shorter than those in CD-MOF-1, wherein the  $\gamma\text{-CD}$  tori are linked by  $\text{K}^+$  ions. In total, each  $\gamma\text{-CD}$  unit is bound to three  $\text{Sr}^{2+}$  cations (Figure 9f).

A topological analysis reveals that the structure of  $[(\text{SrBr}_2) \cdot (\gamma\text{-CD})]_n$  comprises two topologically equivalent three-connected nodes, one based at the centroids of the  $\gamma\text{-CD}$  rings, the other based on the  $\text{Sr}^{2+}$  ions. The resulting network has the Schläfli symbol  $10^3$ , and both nodes have the long vertex symbol  $10_2.10_2.10$ ,

features which define the network as having a  $\text{B}_2\text{O}_3$ , or **bto** net.<sup>47</sup> It is also topologically the same as Wells' (10, 3)- $c$  net,<sup>50</sup> which has previously been reported in two<sup>51</sup> interpenetrated coordination polymeric structures; in one case, it was found as one network component of a heterointerpenetrating structure,<sup>51a</sup> while, in the other, the network may not have been interpreted appropriately.<sup>51b</sup>

Having prepared extended framework structures successfully with  $\gamma\text{-CD}$  and Group IA and IIA metal cations, the natural progression was to investigate the structure directing properties of other (transition) metals cations under similar conditions. Since the hydroxide salts of transition metals and other larger cations are generally insoluble in water, halide salts were employed in all our experiments. Crystals were isolated when MeOH was vapor diffused into aqueous solutions of  $\gamma\text{-CD}$  and the metal salts. Some of the crystals were colored as a result of the inclusion of metal cations, presumably. In all cases, however, X-ray diffraction analysis showed the crystals to contain only  $\gamma\text{-CD}$  in the columnar tetragonal arrangement as observed previously.<sup>21</sup> The color arises, we suspect, from the incorporation of small amounts of metal salts into the crystal, which has pores running along the  $c$  axis; the small fractions of metal cations are disordered and could not be resolved.

The fact that we have not been able to prepare extended frameworks from transition metals under the same conditions as those used for the self-assembly of MOFs with alkali metals suggests that coordinative bonds from the protonated hydroxyl groups of  $\gamma\text{-CD}$  to the metal are not favored. Indeed, examination of structurally characterized complexes of cyclodextrins<sup>52</sup> with transition and heavy metals shows that deprotonation of the CD hydroxyl groups is required in order to form metal-CD bonds, and thus linking the CD tori together.<sup>53</sup>

## CONCLUSION

In the more than 40 years of development of the field of supramolecular chemistry, the coordination of alkali and alkaline earth metal cations by macrocyclic and macrobicyclic hosts composed of  $-\text{OCCO}-$  units has been studied intensively

and extensively. It is perhaps surprising, therefore, that this paradigm has not been extended to the naturally occurring, cyclic oligosaccharides<sup>54</sup> that are the cyclodextrins.<sup>55</sup> We have shown that, by crystallizing the C<sub>8</sub> symmetrical  $\gamma$ -cyclodextrin in aqueous alcohol in the presence of alkali metal salts, compounds with extended frameworks can be isolated. CD-MOF-1 and CD-MOF-2, prepared on the gram-scale from KOH and RbOH, respectively, are defined by a porous, body-centered cubic array of ( $\gamma$ -CD)<sub>6</sub> cubic units which are linked by coordination of the –OCCO– units located on the D-glucopyranosyl residues of  $\gamma$ -CD to the Group IA metal cations. Their robust frameworks are stable to the removal of solvent, and can absorb gases and small organic molecules, with surface areas of approximately 1200 m<sup>2</sup> g<sup>-1</sup>. While additional cubic CD-MOFs have been prepared from a variety of alkali metal salts, the lack of the preorganization of the hard oxygen donor atoms results in the formation of other, topologically distinct, frameworks, including (i) CD-MOF-4, wherein the  $\gamma$ -CD units are arranged in channels and linked by Cs<sup>+</sup> ions, (ii) a two-dimensional sheet structure linked by Na<sup>+</sup> cations, and (iii) a three-dimensional, trigonal framework of  $\gamma$ -CD tori linked by coordination to Sr<sup>2+</sup> cations. It is also possible to prepare edible CD-MOFs entirely from food-grade ingredients. In summary, CD-MOF-1 and CD-MOF-2 show particular promise for technological development as simple, inexpensive, and green porous materials. Moreover, we have demonstrated, in a general and fundamental manner, that the cyclodextrins do indeed act as ligands for Group IA and IIA metal cations in much the same way as do crown ethers, but with a much greater propensity<sup>56</sup> to form extended structures in the solid state. One is left reflecting on the fact that the cubic CD-MOF topology is the one that almost got away!

## ■ ASSOCIATED CONTENT

**S Supporting Information.** Synthesis and characterization of all materials. CCDC 773708–773711 and 853694–853696 contain the supplementary crystallographic data for this paper. These data can be obtained free of charge from the Cambridge Crystallographic Data Centre via [http://www.ccdc.cam.ac.uk/data\\_request/cif](http://www.ccdc.cam.ac.uk/data_request/cif). This material is available free of charge via the Internet at <http://pubs.acs.org>.

## ■ AUTHOR INFORMATION

**Corresponding Author**  
stoddart@northwestern.edu

## ■ ACKNOWLEDGMENT

The research was based in part upon work supported under the auspices of an international collaboration supported in the U.S. by the National Science Foundation under grant CHE-0924620 and in the U.K. by the Engineering and Physical Sciences Research Council under Grant EP/H003517/1. In addition, the authors thank Dr. Turki S. Al-Saud and Dr. Mohamed B. Alfageeh at the King Abdulaziz City for Science and Technology (KACST) in Saudi Arabia for their joint collaborative efforts. The research was also supported by the WCU Program (R31-2008-000-1005) at KAIST in Korea. R.Q.S. gratefully acknowledges support by the Defense Threat Reduction Agency (Grant No. HDTRA1-09-1-0007).

## ■ REFERENCES

- (1) (a) Pedersen, C. J. *J. Am. Chem. Soc.* **1967**, *89*, 2495. (b) Pedersen, C. J. *J. Am. Chem. Soc.* **1967**, *89*, 7017.
- (2) Pedersen, C. J. *Aldrichimica Acta* **1971**, *4*, 1.
- (3) (a) Lehn, J.-M. *Science* **1985**, *227*, 849. (b) Lehn, J.-M. *Angew. Chem., Int. Ed. Engl.* **1988**, *27*, 89. (c) Lehn, J.-M. *Angew. Chem., Int. Ed. Engl.* **1990**, *29*, 1304. (d) Lehn, J.-M. *Supramolecular Chemistry: Concepts and Perspectives*; Wiley VCH: Weinheim, Germany, 1995. (e) Beer, P. D.; Gale, P. A.; Smith, D. K. *Supramolecular Chemistry*; Oxford University Press: Oxford, UK, 1999. (f) Steed, J. W.; Atwood, J. L. *Supramolecular Chemistry*; Wiley VCH: Weinheim, Germany, 2009. (g) Stoddart, J. F. *Nat. Chem.* **2009**, *1*, 14.
- (4) (a) Pedersen, C. J. *J. Am. Chem. Soc.* **1970**, *92*, 386. (b) Pedersen, C. J. *J. Am. Chem. Soc.* **1970**, *92*, 391. (c) Bright, D.; Truter, M. R. *J. Chem. Soc. B* **1970**, 1544. (d) Bush, M. A.; Truter, M. R. *J. Chem. Soc. B* **1971**, 1440. (e) Frensdorff, H. K. *J. Am. Chem. Soc.* **1971**, *93*, 600. (f) Frensdorff, H. K. *J. Am. Chem. Soc.* **1971**, *93*, 4684. (g) Bush, M. A.; Truter, M. R. *J. Chem. Soc., Perkin Trans. 2* **1972**, 341. (h) Bush, M. A.; Truter, M. R. *J. Chem. Soc., Perkin Trans. 2* **1972**, 345. (i) Mallinson, P. R.; Truter, M. R. *J. Chem. Soc., Perkin Trans. 2* **1972**, 1818. (j) Pedersen, C. J.; Frensdorff, H. K. *Angew. Chem., Int. Ed. Engl.* **1972**, *11*, 16. (k) Pedersen, C. J. *Angew. Chem., Int. Ed. Engl.* **1988**, *27*, 1021. (l) Luger, P.; André, C.; Rudert, R.; Zobel, D.; Knöchel, A.; Krause, A. *Acta Crystallogr. Sect. B* **1992**, *48*, 33.
- (5) (a) Cram, D. J.; Cram, J. M. *Science* **1974**, *183*, 803. (b) Cram, D. J. *Science* **1983**, *219*, 1177. (c) Cram, D. J. *Angew. Chem., Int. Ed. Engl.* **1988**, *27*, 1009. (d) Cram, D. J.; Cram, J. M. *Container Molecules and Their Guests*; Royal Society of Chemistry: Cambridge, 1994.
- (6) (a) Dietrich, B.; Lehn, J.-M.; Sauvage, J.-P. *Tetrahedron Lett.* **1969**, 2885. (b) Dietrich, B.; Lehn, J.-M.; Sauvage, J.-P. *Tetrahedron Lett.* **1969**, 2889. (c) Truter, M. R.; Pedersen, C. J. *Endeavour* **1971**, *30*, 142. (d) Moras, D.; Metz, B.; Weiss, R. *Acta Crystallogr., Sect. B* **1973**, *29*, 383.
- (7) (a) Lehn, J.-M.; Sauvage, J.-P.; Dietrich, B. *J. Am. Chem. Soc.* **1970**, *92*, 2916. (b) Lehn, J.-M.; Sauvage, J.-P. *J. Chem. Soc. D, Chem. Commun.* **1971**, 440. (c) Lehn, J.-M.; Sauvage, J.-P. *J. Am. Chem. Soc.* **1975**, *97*, 6700. (d) Kauffmann, E.; Lehn, J.-M.; Sauvage, J.-P. *Helv. Chim. Acta* **1976**, *59*, 1099.
- (8) It should be noted, however, that Cram and Trueblood showed later on the remarkable power of preorganization in host-guest chemistry with the introduction of spherands as geometrically well-defined ligands to act as hosts in the complexation of Groups IA and IIA metal cations. For example, an (OMe)<sub>6</sub>-spherand, even with its six phenolic oxygen atoms, forms exceptionally strong complexes with Li<sup>+</sup>, Na<sup>+</sup>, and Mg<sup>2+</sup> ions by adopting a rigid conformation with close to D<sub>3d</sub> molecular symmetry. See: Cram, D. J.; Trueblood, K. N. *Top. Curr. Chem.* **1981**, *98*, 43.
- (9) Stoddart, J. F. *Chem. Soc. Rev.* **1979**, *8*, 85.
- (10) The log K<sub>a</sub> values for the complexation of KCl in MeOH range from 6.01 through 5.38 and 4.14 to 3.26 for the *cis-syn-cis*, *cis-anti-cis*, *trans-syn-trans*, and *trans-anti-trans* isomers of dicyclohexano[18]crown-6. For more details, see: Coxon, A. C.; Laidler, D. A.; Pettman, R. B.; Stoddart, J. F. *J. Am. Chem. Soc.* **1978**, *100*, 8260.
- (11) (a) Batten, S. R.; Robson, R. *Angew. Chem., Int. Ed.* **1998**, *37*, 1460. (b) Janiak, C. *Dalton Trans.* **2003**, 2781. (c) Kitagawa, S.; Kitaura, R.; Noro, S. *Angew. Chem., Int. Ed.* **2004**, *43*, 2334. (d) Kawano, M.; Fujita, M. *Coord. Chem. Rev.* **2007**, *251*, 2592.
- (12) (a) Cheetham, A. K.; Férey, G.; Loiseau, T. *Angew. Chem., Int. Ed.* **1999**, *38*, 3268. (b) Li, H.; Eddaoudi, M.; O'Keeffe, M.; Yaghi, O. M. *Nature* **1999**, *402*, 276. (c) Eddaoudi, M.; Moler, D. B.; Li, H.; Chen, B.; Reineke, T. M.; O'Keeffe, M.; Yaghi, O. M. *Acc. Chem. Res.* **2001**, *34*, 319. (d) Férey, G. *Chem. Soc. Rev.* **2008**, *37*, 191. (e) Long, J. R.; Yaghi, O. M. *Chem. Soc. Rev.* **2009**, *38*, 1213.
- (13) (a) Szejtli, J. *Chem. Rev.* **1998**, *98*, 1743. (b) Dodziuk, H. *Cyclodextrins and Their Complexes*; Wiley-VCH: Weinheim, 2006.
- (14) Small molecule carbohydrates have long been known to form complexes with Group IA and IIA metal cations. See, for example: (a) Rendleman, J. A., Jr. *Adv. Carbohydr. Chem.* **1966**, *21*, 209.



(b) Angyal, S. J. *Chem. Soc. Rev.* **1980**, 9, 415. (c) Angyal, S. J.; Tipson, S. R.; Horton, D. *Adv. Carbohydr. Chem. Biochem.* **1989**, 47, 1.

(15) (a) Villiers, A. *Compt. Rend. Fr. Acad. Sci.* **1891**, 112, 536. (b) Cramer, F. *Angew. Chem.* **1952**, 64, 136. (c) French, D. *Adv. Carbohydr. Chem.* **1957**, 12, 189. (d) Breslow, R. *Chem. Soc. Rev.* **1972**, 1, 553. (e) Saenger, W. *Angew. Chem., Int. Ed. Engl.* **1980**, 19, 344. (f) Breslow, R. *Science* **1982**, 218, 532. (g) Tabushi, I. *Acc. Chem. Res.* **1982**, 15, 66. (h) D'Souza, V. T.; Bender, M. L. *Acc. Chem. Res.* **1987**, 20, 146. (i) Stoddart, J. F. *Carbohydr. Res.* **1989**, 192, xii. (j) Connors, K. A. *Chem. Rev.* **1997**, 97, 1325. (k) Breslow, R.; Dong, S. D. *Chem. Rev.* **1998**, 98, 1997. (l) Del Valle, E. M. M. *Process Biochem.* **2004**, 39, 1033. (m) Chen, G.; Jiang, M. *Chem. Soc. Rev.* **2011**, 40, 2254.

(16) Bogdan, M.; Caira, M. R.; Farcas, S. I. *Supramol. Chem.* **2002**, 14, 427.

(17) (a) Noltemeyer, M.; Saenger, W. *J. Am. Chem. Soc.* **1980**, 102, 2710. (b) Benner, K.; Klüfers, P.; Schuhmacher, J. *Angew. Chem., Int. Ed. Engl.* **1997**, 36, 743. (c) Benner, K.; Ihringer, J.; Klüfers, P.; Marinov, D. *Angew. Chem., Int. Ed.* **2006**, 45, 5818. (d) Lippold, I.; Vlay, K.; Görls, H.; Plass, W. *J. Inorg. Biochem.* **2009**, 103, 480.

(18) (a) Charpin, P.; Nicolis, I.; Villain, F.; de Rango, C.; Coleman, A. W. *Acta Crystallogr., Sect. C* **1991**, 47, 1829. (b) Chetcuti, P. A.; Moser, P.; Rihs, G. *Organometallics* **1991**, 10, 2895. (c) Caira, M. R.; Griffith, V. J.; Nassimbeni, L. R.; Vanoudtshoorn, B. *J. Chem. Soc., Chem. Commun.* **1994**, 1061. (d) Nicolis, I.; Coleman, A. W.; Charpin, P.; de Rango, C. *Acta Crystallogr., Sect. B* **1996**, 52, 122. (e) Caira, M. R.; Griffith, V. J.; Nassimbeni, L. R. *J. Incl. Phenom. Macro. Chem.* **1998**, 32, 461. (f) Nicolis, I.; Coleman, A. W.; Selkti, M.; Villain, F.; Charpin, P.; de Rango, C. *J. Phys. Org. Chem.* **2001**, 14, 35. (g) Lippold, I.; Görls, H.; Plass, W. *Eur. J. Inorg. Chem.* **2007**, 2007, 1487.

(19) Produced microbiologically on the ton scale from starch (Li, Z. F.; Wang, M.; Wang, F.; Gu, Z. B.; Du, G. C.; Wu, J.; Chen, J. *Appl. Microbiol. Biotechnol.* **2007**, 77, 245), the cyclodextrins have found widespread application (Szejtli, J. *J. Mater. Chem.* **1997**, 7, 575. Hedges, A. R. *Chem. Rev.* **1998**, 98, 2035.) in a variety of commercial arenas, e.g., as food additives (Szente, L.; Szejtli, J. *Trends Food Sci. Technol.* **2004**, 15, 137. Astray, G.; Gonzalez-Barreiro, C.; Mejuto, J. C.; Rial-Otero, R.; Simal-Gandara, J. *Food Hydrocolloids* **2009**, 23, 1631.), in drug formulations (Uekama, K.; Hirayama, F.; Irie, T. *Chem. Rev.* **1998**, 98, 2045. Davis, M. E.; Brewster, M. E. *Nat. Rev. Drug Discovery* **2004**, 3, 1023. Brewster, M. E.; Loftsson, T. *Adv. Drug Delivery Rev.* **2007**, 59, 645) and in cosmetics.<sup>151</sup>

(20) The fact that  $\gamma$ -CD is 8-fold symmetric means that, aside from it having a  $C_8$  axis, it also contains  $C_4$  and  $C_2$  axes. It is this high symmetry, present in a dissymmetric molecule, which makes it such a potent multidentate ligand for Group IA metal cations. A similar situation pertains in  $\alpha$ -CD, where  $C_3$  and  $C_2$  axes commute with its 6-fold symmetry ( $C_6$ ), but not in the case of  $\beta$ -CD, which is out on a limb with its  $C_7$  symmetry, seven being a prime number.

(21) Steiner, T.; Saenger, W. *Acta Crystallogr., Sect. B* **1998**, 54, 450.

(22) Smaldone, R. A.; Forgan, R. S.; Furukawa, H.; Gassensmith, J. J.; Slawin, A. M. Z.; Yaghi, O. M.; Stoddart, J. F. *Angew. Chem., Int. Ed.* **2010**, 49, 8630.

(23) *Preparation of CD-MOF-1.*  $\gamma$ -CD (1.30 g, 1 mmol) and KOH (450 mg, 8 mmol) were dissolved in  $H_2O$  (20 mL). The aqueous solution was filtered and MeOH (ca. 50 mL) was allowed to vapor diffuse into the solution. After 1 week, colorless cubic crystals (1.20 g, 66%), suitable for X-ray crystallographic analysis, were isolated, filtered and washed with MeOH ( $2 \times 30$  mL), before being left to dry in air. Calcd. for  $[(C_{48}H_{80}O_{40})(KOH)_2(H_2O)_8(CH_3OH)_8]_n$ : C, 37.2; H, 7.33. Found: C, 37.2; H, 7.24%. This elemental analysis data corresponds to 22% solvent composition by weight percentage which is commensurate with the TGA data which show a weight loss of ca. 22% at 100 °C. Elemental analysis was also carried out on a dried sample of CD-MOF-1. Calcd. for  $[(C_{48}H_{80}O_{40})(KOH)_2(H_2O)_2]_n$ : C, 39.9; H, 5.80. Found: C, 39.9; H, 6.00%.

(24) *Preparation of CD-MOF-2.*  $\gamma$ -CD (1.30 g, 1 mmol) and RbOH (820 mg, 8 mmol) were dissolved in  $H_2O$  (20 mL). The aqueous solution was filtered and MeOH (ca. 50 mL) was allowed to vapor

diffuse into the solution. After 1 week, colorless cubic crystals (1.25 g, 71%), suitable for X-ray crystallographic analysis, were isolated, filtered and washed with MeOH ( $2 \times 30$  mL) before being left to dry in air. Calcd. for  $[(C_{48}H_{80}O_{40})(RbOH)_2(H_2O)_{11}(CH_3OH)_2]_n$ : C, 34.0; H, 6.40. Found: C, 34.1; H, 6.32%. This elemental analysis data corresponds to 15% solvent composition by a weight percentage which is commensurate with the TGA data that show a weight loss of ca. 15% at 100 °C. Elemental analysis was also carried out on a dried sample of CD-MOF-2. Calcd. for  $[(C_{48}H_{80}O_{40})(RbOH)_2(CH_2Cl_2)_{0.5}]_n$ : C, 37.7; H, 5.42. Found: C, 37.8; H, 5.24%.

(25) *Crystal Data for CD-MOF-1.*  $K_2(C_{48}H_{80}O_{40})(OH)_2$ , colorless cube,  $M_r = 1409.34$ , crystal size  $0.20 \times 0.20 \times 0.20$  mm<sup>3</sup>, cubic, space group  $I432$ ,  $a = 31.006(8)$  Å,  $V = 29807(14)$  Å<sup>3</sup>,  $Z = 12$ ,  $\rho_{calc} = 0.942$  g cm<sup>-3</sup>,  $T = 93(2)$  K,  $\mu = 0.164$  mm<sup>-1</sup>, 152 671 reflections collected, unique reflections, ( $R_{int}$ ) = 4574 (0.0459),  $R_1(F^2 > 2\sigma F^2) = 23.91$ ,  $wR_2 = 0.5723$  (all data).

(26) *Crystal Data for CD-MOF-2.*  $Rb_2(C_{48}H_{80}O_{40})(OH)_2$ , colorless cube,  $M_r = 1502.08$ , crystal size  $0.20 \times 0.20 \times 0.15$  mm<sup>3</sup>, cubic, space group  $I432$ ,  $a = 31.0790(12)$  Å,  $V = 30019(2)$  Å<sup>3</sup>,  $Z = 12$ ,  $\rho_{calc} = 1.082$  g cm<sup>-3</sup>,  $T = 93(2)$  K,  $\mu = 1.046$  mm<sup>-1</sup>, 150 144 reflections collected, unique reflections, ( $R_{int}$ ) = 4609 (0.0836),  $R_1(F^2 > 2\sigma F^2) = 11.4$ ,  $wR_2 = 0.3261$  (all data).

(27) *Preparation of CD-MOF-3/CD-MOF-4.*  $\gamma$ -CD (1.30 g, 1 mmol) and CsOH  $\cdot H_2O$  (1.34 g, 8 mmol) were dissolved in  $H_2O$  (20 mL). The aqueous solution was filtered and MeOH (ca. 50 mL) was allowed to vapor diffuse into the solution during the period of 1 week. Over many different experiments, it was found that crystals of both CD-MOF-3 (cubic blocks) and CD-MOF-4 (needles) separated during the same crystallization procedure. The ratio varied with each experiment, but approximately 1.2 g of mixed material could be recovered. Although the crystals of CD-MOF-3 and CD-MOF-4 could be separated manually, some cross-contamination of the samples was difficult to avoid.

(28) *Crystal Data for CD-MOF-3.*  $Cs_2(C_{48}H_{80}O_{40})(OH)_2$ , colorless cube,  $M_r = 1596.96$ , crystal size  $0.41 \times 0.31 \times 0.05$  mm<sup>3</sup>, cubic, space group  $I432$ ,  $a = 30.868(10)$  Å,  $V = 29411(16)$  Å<sup>3</sup>,  $Z = 12$ ,  $\rho_{calc} = 0.813$  g cm<sup>-3</sup>,  $T = 93(2)$  K,  $\mu = 1.466$  mm<sup>-1</sup>, 152 127 reflections collected, unique reflections, ( $R_{int}$ ) = 4515 (0.0820),  $R_1(F^2 > 2\sigma F^2) = 21.28$ ,  $wR_2 = 0.5285$  (all data).

(29) Blatov, V. A. *IUCr CompComm Newsletter* **2006**, 7, 4.

(30) The unit cell parameters of CD-MOF-1, where the Group IA metal cation is  $K^+$  and which adopts the cubic space group  $I432$  with a unit cell edge of approximately 31 Å, are very similar to some crystallographic data reported in the literature in 2004 for crystals of  $\gamma$ -CD obtained in the presence of  $Na^+$  ions. In this earlier report, addition of an ethanolic solution of NaOH to a DMF solution of  $FeCl_3$  and  $\gamma$ -CD yielded cubic orange single crystals of  $\gamma$ - $Fe_2O_3/\gamma$ -CD. Similar colorless cubic crystals were obtained when NaCl replaced the  $FeCl_3$ . The authors report that they were unable, despite repeated attempts, to solve the solid-state structures of these crystals. It seems more than likely, however, that these crystals constituted cubic CD-MOFs held together by  $Na^+$  ions. See: Bonacchi, D.; Caneschi, A.; Dorignac, D.; Falqui, A.; Gatteschi, D.; Rovai, D.; Sangregorio, C.; Sessoli, R. *Chem. Mater.* **2004**, 16, 2016.

(31) The combination of either LiOH or  $Li_2CO_3$  with  $\gamma$ -CD in aqueous solution, followed by vapor diffusion of MeOH, led to the formation of large colorless crystals in each case. While it was possible to obtain unit cell parameters corresponding to a large hexagonal structure with unit cell edges of 46.2 and 25.7 Å, we were unable to collect data suitable enough to solve the structure. <sup>1</sup>H NMR spectroscopy of  $D_2O$  solutions of redissolved crystals confirmed the presence of  $\gamma$ -CD, and we speculate that these crystals constitute a  $Li^+$  linked framework of some form or other.

(32) Crystalline nanocubes, 300 nm in length, have been reported as the result of dropping an aqueous solution of  $\gamma$ -CD and KI, both present at a concentration of 0.17 M, into isopropanol. Whilst this ratio of  $\gamma$ -CD to KI is less than that present in CD-MOF-1, the powder X-ray diffraction pattern of the nanocubes bears some similarities to that of CD-MOF-1, suggesting that the methodology described above could be



adapted to prepare nanocrystalline CD-MOF-1. See: Marui, Y.; Kida, T.; Akashi, M. *Chem. Mater.* **2010**, *22*, 283.

(33) The crystallographic data sets collected for the CD-MOFs prepared from  $\text{Na}_2\text{CO}_3$ ,  $\text{K}_2\text{CO}_3$ , KF, and  $\text{K}_2(4,4'\text{-azobenedicarboxylate})$  were sufficient to allow us to observe the body-centered cubic framework which defines CD-MOFs 1–3. Although we have, as yet, been unable to refine fully the solid-state structures of these four CD-MOFs to a standard suitable for publication, the data do confirm that these alkali metal salts, in concert with  $\gamma$ -CD, form extended frameworks.

(34) Han, S.; Wei, Y.; Valente, C.; Forgan, R. S.; Gassensmith, J. J.; Smaldone, R. A.; Nakanishi, H.; Coskun, A.; Stoddart, J. F.; Grzybowski, B. A. *Angew. Chem., Int. Ed.* **2011**, *50*, 276.

(35) *Preparation of Edible CD-MOF-1*. Food grade crystals of CD-MOF-1 were prepared by dissolving commercially available food-grade potassium benzoate (283 mg, 1.8 mmol) and food-grade  $\gamma$ -CD (2.30 g, 1.8 mmol) in distilled water. When the aqueous solution was filtered through cotton wool and, following vapor diffusion of Everclear grain alcohol into the solution over a few days, crystals of edible CD-MOF-1 were obtained. Note that  $\gamma$ -cyclodextrin has been declared fit for human consumption. See: Munro, I. C.; Newberne, P. M.; Young, V. R.; Bar, A. *Regul. Toxicol. Pharmacol.* **2004**, *39*, S3.

(36) *Crystal Data for Edible CD-MOF-1*.  $\text{K}_4(\text{C}_{96}\text{H}_{160}\text{O}_{80})(\text{C}_7\text{H}_5\text{O}_2)_2 \cdot 2(\text{OH})_2$ , colorless cube,  $M_r = 3005.17$ , crystal size  $0.40 \times 0.35 \times 0.35 \text{ mm}^3$ , trigonal, space group  $R\bar{3}2$ ,  $a = 31.006(8)$ ,  $c = 28.4636(5) \text{ \AA}$ ,  $\gamma = 120^\circ$ ,  $V = 44842.8(9) \text{ \AA}^3$ ,  $Z = 9$ ,  $\rho_{\text{calc}} = 1.002 \text{ g cm}^{-3}$ ,  $T = 100(2) \text{ K}$ ,  $\mu = 1.466 \text{ mm}^{-1}$ , 69 465 reflections collected, unique reflections, ( $R_{\text{int}} = 14282(0.0515)$ ),  $R_1(F^2 > 2\sigma F^2) = 12.8$ ,  $wR_2 = 0.3814$  (all data).

(37) (a) Li, Q.; Zhang, W.; Miljanić, O. Š.; Sue, C.-H.; Zhao, Y.-L.; Liu, L.; Knobler, C. B.; Stoddart, J. F.; Yaghi, O. M. *Science* **2009**, *325*, 855. (b) Deng, H.; Olson, M. A.; Stoddart, J. F.; Yaghi, O. M. *Nat. Chem.* **2010**, *2*, 439.

(38) In addition, examining the coordination spheres of the  $\text{K}^+$  ions present in the edible MOF revealed K–O bond distances that are commensurate with those of CD-MOF-1, providing further evidence that basic metal salts, such as hydroxides, do not deprotonate the  $\gamma$ -CD units during the formation of CD-MOFs. Indeed, we would not expect deprotonation of the hydroxyl groups ( $\text{p}K_a \approx 13$ ) of  $\gamma$ -CD under the conditions used for self-assembly of CD-MOFs.

(39) Gassensmith, J. J.; Furukawa, H.; Smaldone, R. A.; Forgan, R. S.; Botros, Y. Y.; Yaghi, O. M.; Stoddart, J. F. *J. Am. Chem. Soc.* **2011**, *133*, 15312.

(40) *Crystal Data for CD-MOF-4*.  $\text{C}_{24}\text{H}_{40}\text{CsO}_{20} \cdot \text{OH} \cdot \text{CH}_3\text{OH}$ , colorless prism,  $M_r = 830.52$ , crystal size  $0.3 \times 0.3 \times 0.2 \text{ mm}^3$ , tetragonal, space group  $I4$ ,  $a = 24.136(6)$ ,  $c = 15.454(4) \text{ \AA}$ ,  $V = 9003(4) \text{ \AA}^3$ ,  $Z = 8$ ,  $\rho_{\text{calc}} = 1.226 \text{ g cm}^{-3}$ ,  $T = 93(2) \text{ K}$ ,  $\mu = 0.890 \text{ mm}^{-1}$ , 42 847 reflections collected, unique reflections, ( $R_{\text{int}} = 7891(0.0615)$ ),  $R_1(F^2 > 2\sigma F^2) = 7.99$ ,  $wR_2 = 0.2378$  (all data).

(41) Han, S.; Wei, Y.; Valente, C.; Lagzi, I.; Gassensmith, J. J.; Coskun, A.; Stoddart, J. F.; Grzybowski, B. A. *J. Am. Chem. Soc.* **2010**, *132*, 16358.

(42) (a) Trefry, M. G.; Maslen, E. N.; Spackman, M. A. *J. Phys. Chem. C* **1987**, *20*, 19. (b) Dunitz, J. D.; Bernstein, J. *Acc. Chem. Res.* **1995**, *28*, 193.

(43) Rappé, A. K.; Casewit, C. J.; Colwell, K. S.; Goddard, W. A., III; Skiff, W. M. *J. Am. Chem. Soc.* **1992**, *114*, 10024.

(44) Ewald, P. P. *Ann. Phys.* **1921**, *64*, 253.

(45) Rappé, A. K.; Goddard, W. A., III. *J. Phys. Chem.* **1991**, *95*, 3358.

(46) (a) Giron, D. *Thermochim. Acta* **1995**, *248*, 1. (b) Vipparunta, S. R.; Brittain, H. G.; Grant, D. J. W. *Adv. Drug Delivery Rev.* **2001**, *48*, 3.

(47) O'Keefe, M.; Peskov, M. A.; Ramsden, S. J.; Yaghi, O. M. *Acc. Chem. Res.* **2008**, *41*, 1782.

(48) *Blender*, version 2.58, The Blender Foundation: 2011; www.blender.org.

(49) *Void Analyzer*, version 1.0, Wilmer, C. E.; Snurr, R. Q.; www.chriswilmer.com/pdfs/voidanalyzer.pdf.

(50) Wells, A. F. *Three-Dimensional Nets and Polyhedra*; John Wiley & Sons: New York, 1977.

(51) (a) Zhang, S. S.; Zhan, S. Z.; Li, M.; Peng, R.; Li, D. *Inorg. Chem.* **2007**, *46*, 4365. (b) Huang, Y. J.; Song, Y. L.; Chen, Y.; Li, H. X.; Zhang, Y.; Lang, J. P. *Dalton Trans.* **2009**, 1411.

(52) (a) Fuchs, R.; Habermann, N.; Klüfers, P. *Angew. Chem., Int. Ed. Engl.* **1993**, *32*, 852. (b) Klüfers, P.; Schuhmacher, J. *Angew. Chem., Int. Ed. Engl.* **1994**, *33*, 1863. (c) Klüfers, P.; Piotrowski, H.; Uhlendorf, J. *Chem.—Eur. J.* **1997**, *3*, 601. (d) Geisselmann, A.; Klüfers, P.; Kropfgans, C.; Mayer, P.; Piotrowski, H. *Angew. Chem., Int. Ed.* **2005**, *44*, 924. (e) Benner, K.; Ihringer, J.; Klüfers, P.; Marinov, D. *Angew. Chem., Int. Ed.* **2006**, *45*, 5818. (f) Li, S. L.; Lan, Y. Q.; Ma, J. F.; Yang, J.; Zhang, M.; Su, Z. M. *Inorg. Chem.* **2008**, *47*, 2931.

(53) Norkus, E. J. *Incl. Phenom. Macro. Chem.* **2009**, *65*, 237.

(54) There is now available for investigation an extensive range of synthetic cyclic oligosaccharides (Gattuso, G.; Nepogodiev, S. A.; Stoddart, J. F. *Chem. Rev.* **1998**, *98*, 1919), some of which could well form complexes, if not extended structures, with alkali metal cations. Many of these unnatural cyclodextrins, however, contain rhamnopyranosyl (i.e., 6-deoxy-mannopyranosyl) residues and so those binding sites, where hydroxymethyl groups and glycosidic ring oxygen atoms would normally participate as bidentate ligands towards Group IA metal cations, would be rendered null and void.

(55) So far, although we have not been able to obtain any crystals from aqueous, methanolic solutions of  $\beta$ -CD with added alkali metal salts, we have indeed obtained some crystalline samples when employing  $\alpha$ -CD. The structures of these crystals are under investigation presently by X-ray crystallography.

(56) Simple crown ethers are known to form extended polymeric arrays with Group IA and IIA metal cations. For example, [15]crown-5 forms a 2:1 sandwich-type complex with  $\text{K}^+$  ions, and [12]crown-4 forms a sandwich complex with  $\text{Li}^+$  ions.<sup>4</sup>